Supporting Information

Nickel oxide nanoparticles for efficient hole transport in p-i-n and n-i-p perovskite solar cells

Zonghao Liu [a,b,†], Aili Zhu [a,†], Fensha Cai [a], LeiMing Tao [a], Yinhua Zhou [a], Zhixin Zhao [a,], Qi Chen [c], Yi-Bing Cheng [a,d], Huanping Zhou [b,*]*

[a] Wuhan National Laboratory for Optoelectronics, School of Optical and Electronic Information, Huazhong University of Science and Technology, Wuhan, Hubei 430074, P.R. China

[b] Department of Materials Science and Engineering, College of Engineering, Peking University, Beijing 100871, P. R. China

[c] Department of Materials Science and Engineering, Beijing Institute of Technology, Beijing 100081, P. R. China

[d] Department of Materials Engineering, Monash University, Victoria 3800, Australia

[†] These authors contributed equally to this work.

* Corresponding author:

Z. Zhao (zhixin-zhao@hust.edu.cn);

H. Zhou (hpzhou@pku.edu.cn).

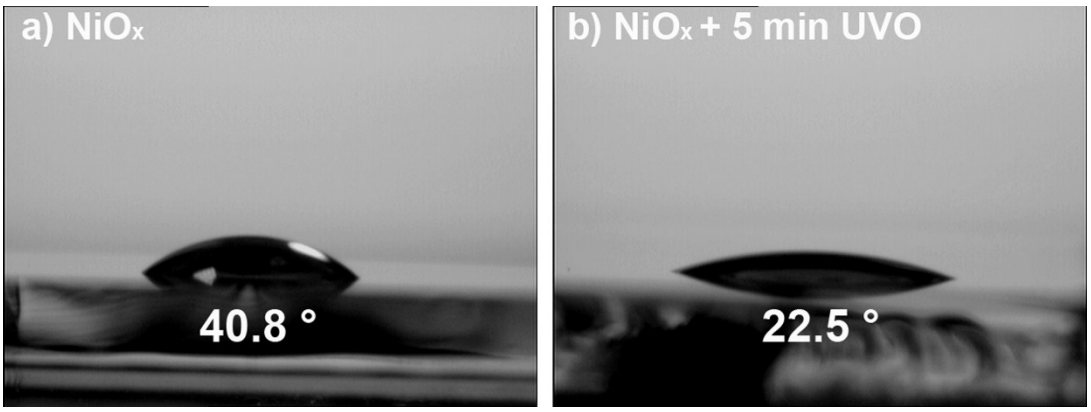

Figure S1 Photographs of the contact angle for the pristine NiO_x and NiO_x with 5 min UVO treatment.

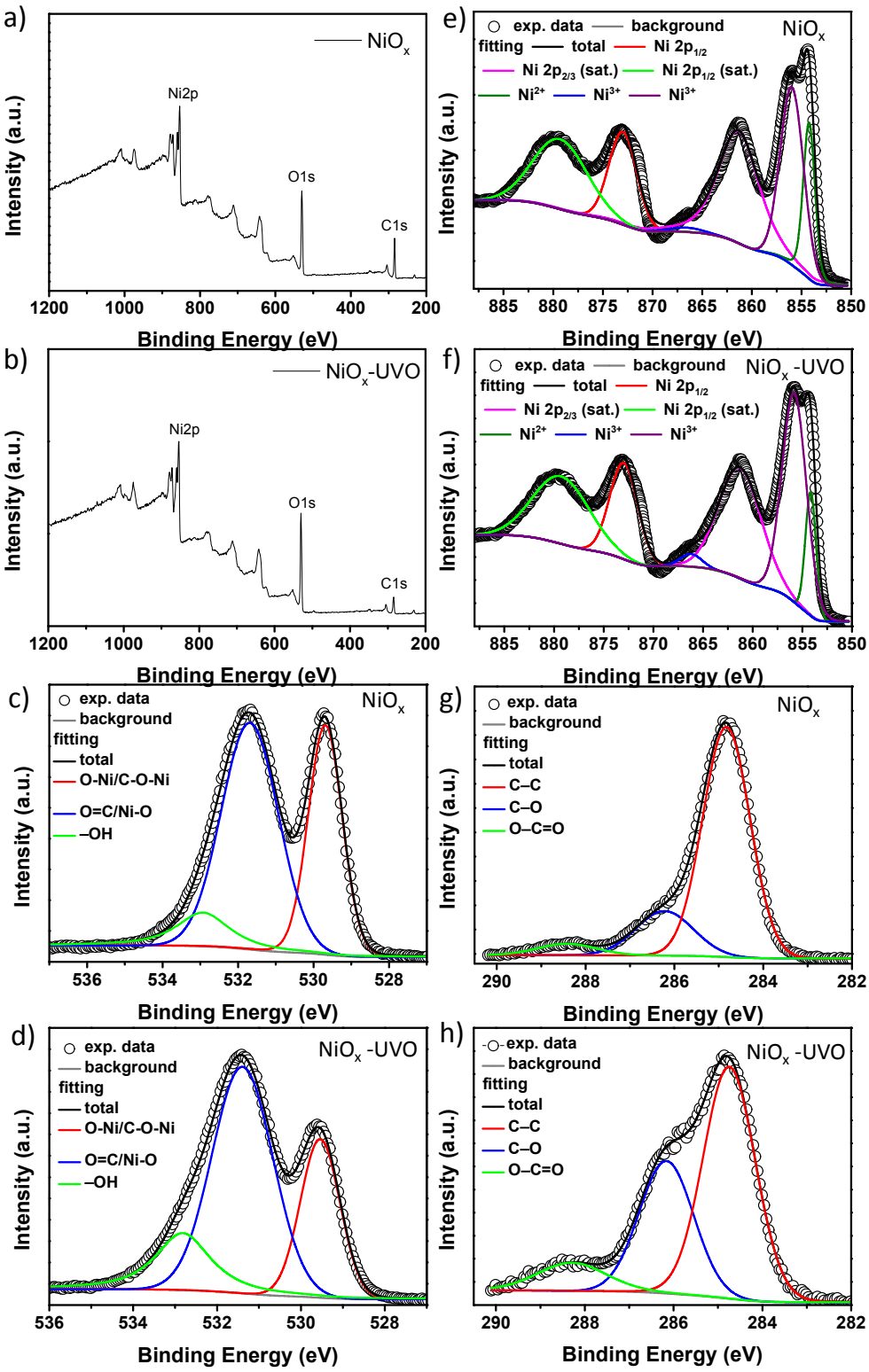

Figure S2. XPS spectra of NiO_x and NiO_x-UVO films. (a-b) survey scan. (c-d) Ni 2p scan. (e-f) O 1s narrow scan. (g-h) C 1s narrow scan.

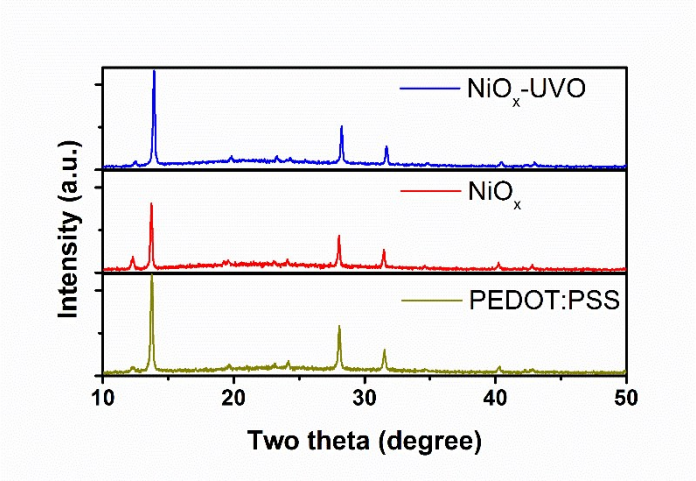

Figure S3 X-ray diffraction patterns of perovskite films upon NiO_x, NiO_x-UVO and PEDOT:PSS substrate, respectively.

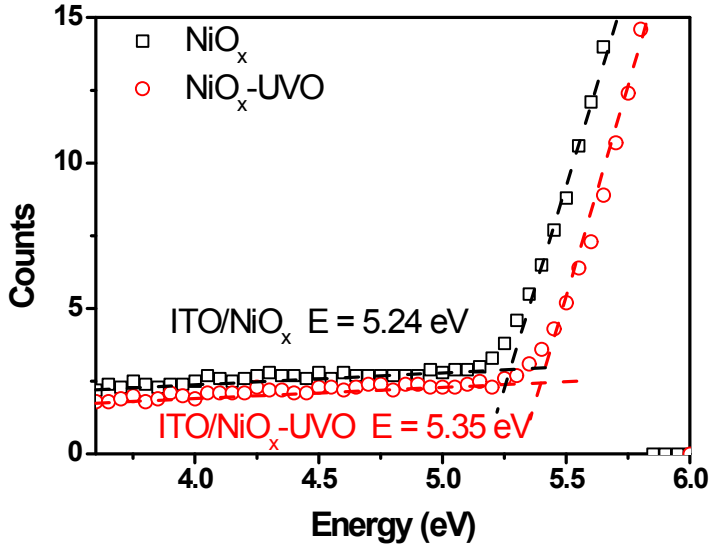

Figure S4 Work function of ITO/NiO_x and ITO/NiO_x-UVO samples measured with UPS.

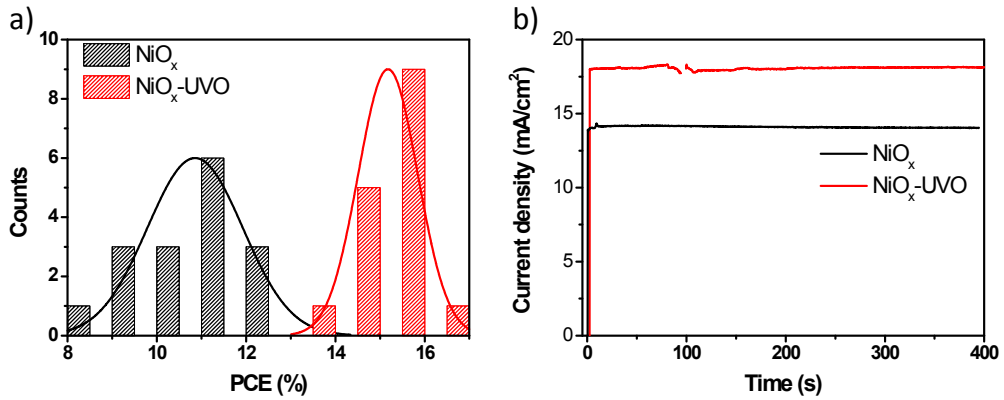

Figure S5 a) Power conversion efficiency distribution for 16 devices measured under standard one sun AM 1.5G simulated solar irradiation. b) Stabilized output measurements: current density as a function of time for the NiO_x based device (0.82 V) and NiO_x-UVO based device (0.87 V) held at a forward bias of maximum output power point.

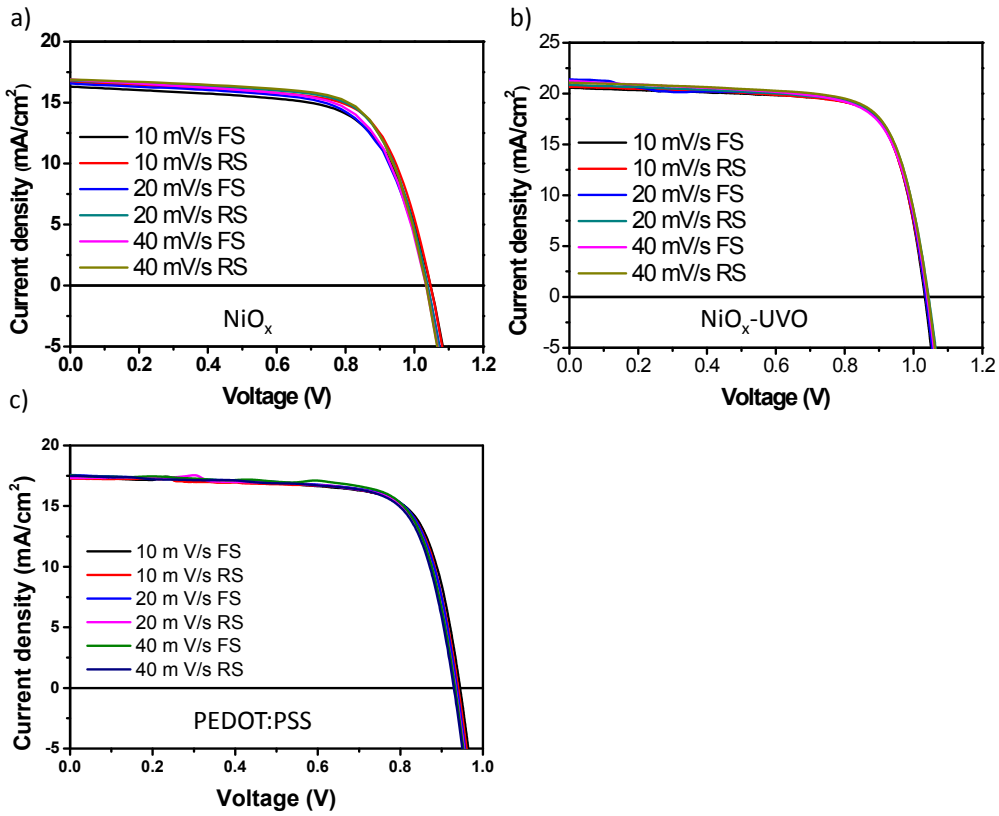

Figure S6 J-V curve of NiO_x (a), NiO_x-UVO (b) and PEDOT:PSS (c) based device measured under different directions (forward scan, FS, from -0.2 V to 1.2 V, reverse scan, RS, from 1.2 V to -0.2 V) and different scan rate (10, 20, 40 mV s^{-1}, respectively).

Table S1 Device performance of the NiO_x, NiO_x-UVO and PEDOT:PSS devices measured under simulated AM 1.5 (100 mW cm^{-2}) conditions with under different directions (forward scan, FS, from -0.2 V to 1.2 V, reverse scan, RS, from 1.2 V to -0.2 V) and different scan rate (10, 20, 40 mV s^{-1}, respectively).

Device	scan direction	scan rate (mV s^{-1})	Voc (V)	Jsc (mA cm^{-2})	FF (%)	PCE (%)
NiO_x-UVO	FS	10	1.03	20.58	74.7	15.89
	RS	10	1.03	20.66	74.2	15.90
	FS	20	1.04	21.41	72.3	16.03
	RS	20	1.04	20.87	73.6	16.04
	FS	40	1.04	21.26	71.4	15.82
	RS	40	1.04	21.08	73.6	16.20
NiO_x	FS	10	1.04	16.31	66.1	11.30
	RS	10	1.04	16.73	68.4	12.00
	FS	20	1.04	16.56	66.3	11.41
	RS	20	1.04	16.83	69.0	12.06
	FS	40	1.04	16.89	66.5	11.62
	RS	40	1.04	16.89	69.6	12.18

PEDOT:PSS	FS	10	0.948	17.38	74.14	12.22
	RS	10	0.938	17.26	75.37	12.20
	FS	20	0.936	17.55	74.61	12.26
	RS	20	0.936	17.33	74.91	12.16
	FS	40	0.916	17.59	76.77	12.37
	RS	40	0.916	17.45	75.64	12.10

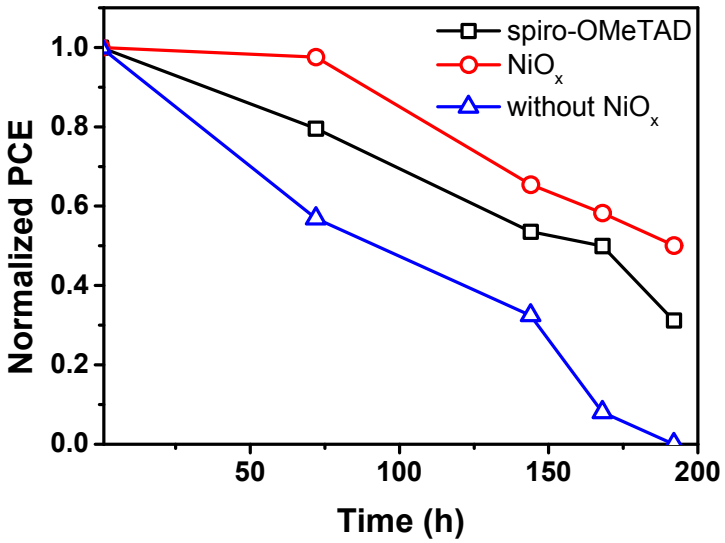

Figure S7 The efficiency of unencapsulated devices stored in ambient air with the humidity of 45−50% under dark.

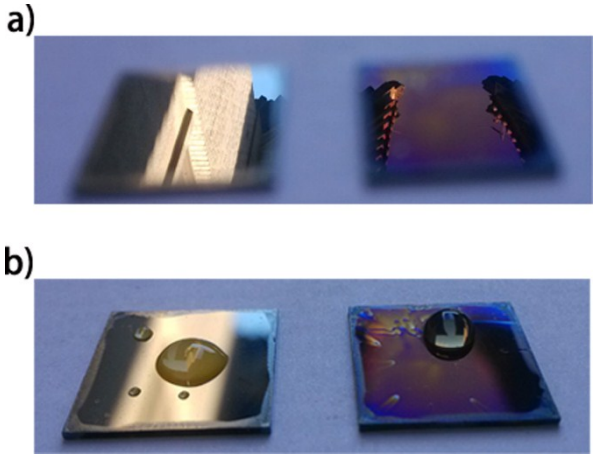

Figure S8 The images of water drop on the surface of perovskite layer and perovskite/NiO_x layer 1 min later.